Journal of Clinical Toxicology
ISSN: 2161-0495

Flores et al., J Clin Toxicol 2016, 6:5
DOI: 10.4172/2161-0495.1000318

Research Article Open Access

# THS Toxins Induce Hepatic Steatosis by Altering Oxidative Stress and SIRT1 Levels

**Cristina Flores, Neema Adhami and Manuela Martins-Green***

*Department of Cell Biology and Neuroscience, University of California, USA*

***Corresponding author:** Manuela Martins-Green, Department of Cell Biology and Neuroscience, BSB room 2217 900 University Avenue, University of California Riverside, Riverside, CA 92521, USA, Tel: 1-951-827-2585; Fax: 1-951-827-3087; E-mail: manuela.martins@ucr.edu

**Received date:** June 21, 2016; **Accepted date:** September 17, 2016; **Published date:** September 22, 2016



## Abstract

**Background:** Third hand smoke (THS) forms when second hand smoke (SHS) tobacco toxins accumulate on surfaces such as walls, carpets and clothing and can result in adverse health effects.

**Objective:** This study was designed to investigate the mechanism of THS-induced hepatic steatosis.

**Methodology:** We used an *in vivo* exposure system that mimics exposure of humans to THS to investigate the effects of THS on hepatic lipid metabolism. THS-exposed mice were treated either with the liver-damaging drug, N-acetyl-p-aminophenol (APAP/Tylenol) to increase oxidative stress or with the antioxidants N-acetyl-cysteine and α-Tocopherol which decrease oxidative stress.

**Results:** THS-exposed mice have higher levels of superoxide dismutase activity and $H_2O_2$ levels. However, no significant changes in activity of the antioxidant enzymes catalase and glutathione peroxidase were found, implying the presence of high levels of hydrogen peroxide in the liver. Furthermore, THS-exposed mice also have a lower NADP+/NADPH ratio, indicating decreased ability of these mice to combat oxidative stress. THS-exposed mice show a decrease in ATP production, increase in aspartate aminotransferase (AST) activity, as well as increased molecular damage (lipid peroxidation, protein nitrosylation and DNA damage). Treating THS-exposed mice with APAP/Tylenol enhances the THS-induced damage whereas treating with antioxidants reduces the damage. THS-exposed mice also have lower sirtuin 1 (SIRT1) levels compared to controls which decreased activation of 5' AMP-activated protein kinase (AMPK) and increased sterol regulatory element binding protein 1c (SREBP1c).

**Conclusion:** THS-exposed mice on a normal diet have increased oxidative stress and damage mediated by oxidative stress, which results in alterations to the SIRT1/AMPK/SREPB1c signaling pathway. Increasing oxidative stress results in enhanced THS-induced damage whereas decreasing oxidative stress causes improvement in the THS-induced liver damage. Our results show that THS is a new risk factor contributing to the development of liver steatosis and highlight the danger of THS in general.

**Keywords:** Lipid metabolism; NAFLD; AMPK; Triglycerides; Antioxidants; SREPB1c; Hepatocyte damage

## Introduction

Third hand smoke (THS) forms when second hand smoke (SHS) tobacco toxins accumulate on surfaces such as walls, carpets and clothing [1-4]. Moreover, these toxins have the ability to react with gases in the air, such as nitrous acid, and produce dangerous carcinogens [5-9]. Individuals are exposed to THS toxins when they come into contact with the deposited toxins or when the toxins are re-emitted into the air. Exposure to THS toxins can result in detrimental health outcomes in individuals who are chronically exposed to them [10-17]. These health effects vary from metabolic disorders to cognitive perturbations. Children are one of the sectors of the population that is most susceptible to tobacco toxins and studies have shown that tobacco metabolites are detected in their urine [13-15]. Unfortunately, this dangerous exposure continues. In 2007, about 5.5 million children lived in households where someone smoked inside the home [12]. Even in households where indoor smoking was not reported, the tobacco metabolites could still be detected in the children's urine [13-15].

Studies in vitro have shown that THS is toxic to human cells. When a liver cell line, HepG2 cells, was exposed to THS toxins their DNA integrity and stability was compromised [16]. Both acute and chronic THS exposure resulted in double strand DNA breaks [16]. These investigators also showed that the molecular damage observed in HepG2 cells was associated with the increase in cellular oxidative stress and therefore suggested that oxidative stress is a major contributor to THS-mediated toxicity in vitro [16]. Another in vitro study focused on the effects of THS in the development of the lung using fetal rat lung explants [17]. These investigators showed that when fetal rat lungs were exposed to the THS toxins nicotine, 1-(N-methyl-N-nitrosamino)-1-(3-pyridinyl)-4butanal (NNA), or 4- (methylnitrosam--ino)-1-(3-pyridyl)-1-butanone (NNK), there was a disruption in the development of alveolar interstitial ibroblasts and that the disruption occurred via down regulation of PPAR-γ signaling [17]. PPAR-γ signaling controls alveolar development and down regulation of this signaling in the lungs suggested a disruption in alveolar epithelial-mesenchymal paracrine signaling, which prevents

normal lung development. Exposure to THS toxins also resulted in increase of fibronectin and calponin protein levels as well as increase in apoptosis, which are markers for abnormal lung development. Together these findings suggest that the lungs of rats exposed to THS toxins do not develop normally, highlighting the danger of exposure to these toxins during lung development.

It also has been shown that THS toxins have the ability to cause metabolic changes in two male germ cell lines [18]. When spermatogonia (GC-2) and sertoli derived cells (TM-4) were exposed to THS toxins for 24 hours, the investigators observed changes in metabolic enzymes involved in glutathione, ammonia and nucleic acid metabolism [18]. In GC-2 cells, THS exposure resulted in increase in synthesis and decrease in the breakdown of GSH. GSH is a major component of the antioxidant defense pathway and these findings suggest spermatogonia might use this enzyme to combat the high levels of oxidative stress [18]. In TM-4 cells, there are increased metabolites involved in nucleic acid metabolism, suggesting that THS toxins are genotoxic and have the ability to compromise the integrity of genetic material [18]. THS exposure did not have effects on cell viability, cell cycle or apoptosis in these two male germ cell lines [18]. However, this in vitro study highlighted the sensitivity of male germ cells to THS toxins.

In addition to the findings *in vitro*, the detrimental effects of THS toxins have also been shown to alter human behavior. Epidemiological studies have shown that THS exposure results in abnormal cognitive function in children [19]. Children exposed to THS toxins are more hyperactive than children that live in environments with less THS contamination. Also, children are exposed to higher levels of these toxins than adults because they are in closer contact with the contaminated surfaces, lick their fingers and their surface-to-volume ratio is larger [19,20]. In addition, they are also more susceptible because their liver is not fully developed and therefore is not as effective in detoxification of toxins. Also, smoking during pregnancy or after pregnancy is dangerous for the developing fetus and results in impaired lung function [21,22]. Post-natal exposure to THS toxins also results in increased problems with the larynx, trachea and bronchi. This resulted in increased cough-and-asthma related symptoms in these children, suggesting THS toxins are detrimental for lung health of children living in homes contaminated with THS toxins.

We have developed an *in vivo* THS exposure system of mice that mimics THS exposure in humans [23]. Our model is a novel exposure system that allows us to study the effects of long-term THS exposure in different organs of male C57BL/6 mice. Using this exposure method, we have shown that THS exposure leads to lipid accumulation in the liver of these mice, suggesting that they have abnormal metabolism and insulin resistance [23,24]. These findings suggest that THS exposure is a new risk for hepatic steatosis.

Hepatic steatosis is the earliest stage of and a hallmark of non-alcoholic liver disease (NAFLD), which is the most common liver disease worldwide [25,26]. In some patients, steatosis can progress into fibrosis and then to cirrhosis if is not treated early. In the U.S., the prevalence of NAFLD is estimated to be around 20% in the general population and the percentage quadruples in morbidly obese individuals [25,26]. NAFLD is not limited to adults; the incidence of NAFLD among the pediatric population is increasing and it is estimated to account for about 14% of all NAFLD cases [25,26]. NAFLD is a complex process that results from metabolic abnormalities [27,28]. Many patients show dyslipidemia, malfunction of beta oxidative enzymes, deficiency in lipoproteins, and immune dysregulation [29,30]. Obesity, metabolic disorders, drugs or smoking are some of the major risk factors contributing to the development of NAFLD [31-33]. This disease is primarily controlled through changes in life-style, cessation of chemical exposure or antioxidant treatments [34-36].

In this study, we performed cellular and molecular studies to investigate whether THS exposure leads to increased oxidative stress in liver, leading to abnormal lipid metabolism and resulting in hepatic steatosis. Here, we show that mice exposed to THS toxins have altered oxidative stress in the liver. Increasing oxidative stress by treating the mice with N-acetyl-p-aminophenol (APAP/Tylenol) leads to exacerbation of THS-induce hepatic steatosis whereas antioxidant treatment ameliorates this condition. These findings suggest that oxidative stress caused by THS toxins leads to lipid accumulation in the liver. More specifically, THS toxins alter the SIRT1/AMPK/SREPB1c pathway, which regulates lipid metabolism in the liver, suggesting, that THS toxins are a new risk factor for development of hepatic steatosis.

## Materials and Methods

### Animals

Male C57BL/6 mice were divided into control and experimental groups (THS-exposed mice). The experimental group was exposed to THS toxins after weaning for 24 weeks. The control group was never exposed to THS toxins. Both control and THS-exposed mice were maintained under controlled environmental conditions -12-hr light/dark cycle in conventional cages with *ad libitum* access to standard chow (percent calories: 58% carbohydrate, 28.5% protein, and 13.5% fat) and water.

### Ethics statement

All animal experimental protocols were approved by the University of California, Riverside, Institutional Animal Care and Use Committee (UCR-IACUC). Mice were euthanized by carbon dioxide ($CO_2$) inhalation, which is the most common method of euthanasia used by NIH. The amount and length of $CO_2$ exposure were approved by UCR-IACUC.

### THS exposure method

Common household fabrics such as curtain material, upholstery and carpet were placed in empty mouse cages and exposed to SHS generated by the a Teague smoking machine as previously described in [23]. Each cage contained 10 g of curtain material (cotton) 10 g of upholstery (cotton and fiber) and two 16 in 2 pieces of carpet (fiber) to maintain equal exposure levels across all experimental groups. Two packs of 3R4F research cigarettes were smoked each day, five days per week to mimic an intermittent smoker. The smoke was routed to a mixing compartment to mix with air and the mixture distributed between two exposure chambers, each containing eight cages with the materials. The gravimetric method was used to determine the total particulate concentrations in each smoke chamber. The weight of Whatman grade 40 quantitative cellulose filter papers was recorded before introducing the filter paper into the filtering device and the device was then allowed to run for 15 minutes. After 15 minutes, the filter was weighed again to determine the particulate mass that had accumulated during this time period. This procedure was repeated with two more filters and the average of the three masses gave the TPM

values for each chamber. The TPM values were adjusted to 30 μg/$m^3$, which resembles the values found in the homes of smokers by the EPA.

All cigarettes were smoked and stored in accordance with the Federal Trade Commission (FTC) smoking regimen. At the end of each week, cages were removed from the exposure chamber, bagged, and transported to the vivarium where mice were placed into the cages with the THS exposed material. For the next week, an identical set of cages and fabric was prepared and exposed to smoke in the same way as the first set of cages. By using two sets of cages and materials, each of which was exposed on alternating weeks, we ensured that mice inhabited cages containing fabric that had been exposed to fresh SHS in the beginning of each week and aged smoke towards the end week. Throughout the exposure period, hair was removed from the backs of the exposed mice (and controls) to mimic the bare skin of humans.

### N-acetyl-p-aminophenol (APAP/Tylenol) treatment

Four cohorts of male mice of the same age were used for *in vivo* APAP treatment studies. APAP was purchased from Sigma (Cat# A5000-100G) and was dissolved in warm PBS and injected IP. THS-exposed mice and controls received a daily dose of 300 mg/kg for eight weeks via IP injections. The concentration of each APAP solution was adjusted so that all mice received approximately the same volume.

### Antioxidant therapy

Four cohorts of male mice, control and THS-exposed, were given antioxidants daily starting at weaning (3 weeks of age) for five months. We used N-acetylcysteine (NAC) and α-tocopherol (α-TOC). NAC (50 mg/kg) was dissolved in PBS and injected daily via IP. α-TOC (150 mg/kg) was dissolved in 70% ethanol and also injected IP daily.

### Tissue extracts

After six months of THS exposure, livers were extracted from THS-exposed or control mice, washed with PBS and immediately frozen. The frozen livers were stored at -80°C. Liver tissue was homogenized in radioimmunoprecipitation assay buffer (RIPA), centrifuged, and the supernatant collected unless otherwise specified by instruction manuals of the assay kits used in this study. Extracts were used to perform the various assays we used for this study.

### Blood extracts

Blood was extracted directly from the heart and allowed to coagulate on ice for 20-30 minutes. The samples were then centrifuged at 10,000 rpm for phase separation. The serum was used immediately for assays or frozen and stored at -80° C and later used in assays.

### Measurement of SOD activity

Cayman Superoxide Dismutase Assay Kit (Cat # 706002) was used to measure SOD levels in the liver. Frozen liver pieces (10 mg) were placed in ice-cold RIPA buffer containing 50 mM Tris (50 mM pH 7), NaCl (150 mM), SDS (0.1%), sodium deoxycholate (0.5%) and Triton X (1%) and homogenize using a Bullet Blender Homogenizer to extract total protein. The samples were centrifuged at 10,000 rpm for 15 min at 4°C, and the resulting supernatant was used for SOD activity assay. Protein quantification was done using the Bradford assay (Bio-Rad). SOD activity was quantified by measuring the dismutation of superoxide radicals generated by xanthine oxidase and hypoxanthine. A standard curve was generated and used to quantify the activity of SOD in the liver samples.

### Measurements of hydrogen peroxide levels

A Cayman Hydrogen Peroxide Assay Kit (Cat # 600050) was used to measure $H_2O_2$ levels in the liver. Fresh liver samples (10 mg) were homogenized in ice-cold RIPA buffer containing 50 mM Tris (50 mM pH 7), NaCl (150 mM), SDS (0.1%), sodium deoxycholate (0.5%) and Triton X (1%) using a Bullet Blender Homogenizer to extract total protein. The samples were centrifuged at 10,000 rpm for 15 min at 4°C, and the resulting supernatant was collected for the assay. $H_2O_2$ was detected using 10-acetyl-3,7-dihydroxyphenoxazine (ADHP), a highly sensitive and stable probe for $H_2O_2$. In the presence of horseradish peroxidase, ADHP reacts with $H_2O_2$ in a 1:1 stoichiometry ratio to produce a highly fluorescent resorufin (excitation=530-560 nm; emission=590 nm). The standard curve generated was used to quantify the activity of hydrogen peroxide in the liver.

### Measurement of catalase activity

Cayman Catalase Assay Kit was used to measure catalase (Cat # 707002) activity. Frozen liver pieces (10 mg) were placed in ice-cold RIPA buffer containing 50 mM Tris (50 mM pH 7), NaCl (150 mM), SDS (0.1%), sodium deoxycholate (0.5%) and Triton X (1%) and homogenized using a Bullet Blender Homogenizer to extract total protein. The samples were centrifuged at 10,000 rpm for 15 minutes at 4°C, and the resulting supernatant was collected and used for the assay. 20 μl of tissue homogenate were added to the wells of a 96 well plate along with 100 μl of assay buffer and 30 μl methanol and the reaction initiated by addition of 20 μl $H_2O_2$. After incubation for 20 mins, 30 μl of potassium hydroxide was added to terminate the reaction. 30 μl of 4-amino-3-hydrazino-5-mercapto-1,2,4-triazole (purpald), which is a chromogen, was added. After incubation for 10 minutes at RT, 10μl potassium periodate was added and incubated again at RT for five minutes. Absorbance was read at 540 nm. The method is based on the reaction of the enzyme with methanol in the presence of an optimal concentration of $H_2O_2$. The formaldehyde produced was measured spectrophotometrically with 4- amino-3-hydrazino-5-mercapto-1,2,4-triazole (Purpald) as the chromogen. Purpald specifically forms a bicyclic heterocycle with aldehydes which, upon oxidation, changes from colorless to a purple color. The amount of catalase activity levels were calculated and standardized for protein using the Bradford method (Bio-Rad).

### Measurements of GPx activity

Cayman GPx activity assay kit (Cat # 703102) was used to measure GPx (Cat # 703102) activity in the liver. Frozen liver pieces (10 mg) were homogenized in ice-cold RIPA buffer containing 50 mM Tris (50 mM pH 7), NaCl (150 mM), SDS (0.1%), sodium deoxycholate (0.5%) and Triton X (1%) using a Bullet Blender Homogenizer to extract total protein. The samples were centrifuged at 10,000 rpm for 15 minutes at 4°C, and the resulting supernatant was collected and used for the assay. 20 μl of liver homogenate were added to the wells of a 96 well plate along with 100 μl of assay buffer and 50 μl of co-substrate composed of NADPH, glutathione and glutathione reductase. Reactions were initiated by addition of hydro peroxide, mixed for a few seconds, and absorbance was read at 340 nm every minute to obtain at least 5 time points. The assay measured GPx activity indirectly by a coupled reaction with glutathione reductase (GR). Oxidized glutathione (GSSG), produced upon reduction of an organic hydroperoxide by

GPx, was recycled to its reduced state by GR and NADPH. The oxidation of NADPH to NADP+ was accompanied by a decrease in absorbance at 340nm. The rate of decrease in the A340 was directly proportional to the GPx activity in the liver homogenate samples.

### Measurement of DNA damage

DNA damage was measured using an ELISA Kit from Cell BioLabs Inc (Cat # STA-320) which allows the quantification of 8-hydroxy-2-deoxy Guanosine (8-OH-dG), DNA damage marker in ng/ml. DNA was extracted from liver samples, dissolved in water (1-5 mg/mL) and converted into single stranded DNA by incubating the sample at 95°C for five minutes following by chilling on ice. DNA was digested to nucleosides by incubating the denatured DNA with 5-20 units of nuclease P1 for 2 hours at 37°C at final concentration of 20 mM Sodium Acetate, pH 5.2, followed by treatment with 5-10 units of alkaline phosphatase for 1 hr at 37°C in a final concentration of 100 mM Tris, pH 7.5. The reaction mixture was centrifuged for five minutes at 6,000 rpm and the supernatant used for the 8- OH-dG ELISA assay. 50 µL of experimental samples or 8-OHdG standards were added to the wells of the 8-OHdG Conjugate coated plate. Incubation was performed at room temperature for 10min on an orbital shaker. 50 µL of anti-8-OHdG antibody was added to each well and the plate was incubated at room temperature for 1hr. The microwells were then washed three times with Wash Buffer. After the last wash, 100 µL of secondary Antibody-Enzyme Conjugated was added and incubation was performed at room temperature for 1 hr followed by three washes. 100 uL of Substrate Solution containing 3,3', 5,5'Tetramethylbenzidine was added to each well and incubated at room temperature for 30 minutes. The enzyme reaction was stopped by addition of 100 µL of Stop Solution into each well. Absorbance was read on a spectrophotometer at λ=450 nm.

### Measurement of nitrosylation of proteins

Protein damage was quantified by measuring the nitrosylation of tyrosine residues in proteins. The amount of 3-nitrotyrosine in the liver proteins was determined using the OxiSelect Nitrotyrosine ELISA Kit from Cell Biolabs (Cat # STA-305). The liver samples or nitrated BSA standards were first added to a nitrated BSA pre-absorbed enzyme immunoassay (EIA) plate. After a brief incubation, an anti-nitrotyrosine antibody was added, followed by an HRP conjugated secondary antibody. The protein nitrotyrosine content in the liver samples were determined by comparing with a standard curve that was prepared from predetermined nitrated BSA standards provide in the kit.

### Measurement of lipid peroxidation

Lipid peroxidation in the liver was determined by the levels of the byproduct of lipid peroxidation known as malaldehyde (MDA) using the OxiSelect TBARS Assay Kit from Cell Biolabs (Cat # STA-330). The unknown MDA containing samples or MDA standards were first reacted with Thiobarbituric Acid (TBA) at 95°C for 60 minutes. After this incubation period, the plate containing the samples and standards was read fluorometrically at 540 nm excitation and 590 nm emission. The MDA content in unknown samples was determined by comparison with the predetermined MDA standard curve.

### Measurement of AST levels

The AST levels were measured using the Aspartate aminotransferase (AST) Activity Assay (Cat# MAK055). 100 uL of the reaction mix (80 uL AST Assay buffer; 2 uL AST enzyme mix; 8 uL AST developer; 10 uL AST substrate) was added to each well. The plate was then mixed by pipetting and incubated at 37°C and was protected from light. The first initial reading was taken after 2 minutes of incubation. After the recording of the first initial reading, the subsequent readings were taken every five minutes until the measurements of the samples where greater than the value of the highest standard (~10 nmole/well). The background in the wells was corrected by subtracting the final reading of standard zero from all the final readings of the eight standards. The standards were then used to make a standard curve. The AST activity was calculated by subtracting the final reading of each sample from initial reading divided by the reaction rate and volume of the sample.

### Measurement of ATP levels

The ATP levels in liver were quantified using BioVision's ATP Colorimetric and Fluorometric Assay kit (Cat # K354-100), which is designed to detect low quantities of ATP (~50 pmol) by measuring the phosphorylation of glycerol. The assay was performed according to the protocol included in the kit. Liver tissue samples (10 mg) were homogenized in 100 µl of ATP assay buffer and 50 µl of sample supernatant was added to a 96-well plate in duplicates. 50 µl of the Reaction Mix (44 µl ATP Assay buffer; 2 µl ATP probe; 2 µl ATP converter; and 2 µl developer) was added to each well containing the ATP standards and samples to initiate the phosphorylation of glycerol reaction. The plate was mixed well and incubated for 30 minutes at room temperature away from light. During this incubation period, glycerol was phosphorylated. The product of this phosphorylation reaction was read at λ=570 nm and the absorbance readings of the standards were used to generate a standard curve. The unknown amount of ATP in the samples was then calculated using the standard curve and the observances reading of the samples.

### Measurement of Urea levels

Urea levels in the liver tissue were quantified using Cell Biolabs' Urea Assay Kit (Cat # STA-382), which is based on the Berthelot reaction. The enzyme urease is used to catalyze the hydrolysis of urea into carbon dioxide and ammonia. Ammonia then reacts with the alkaline developer (Berthelot's reagent) included in this kit to produce a blue-green colored product that can be measured with a standard spectrophotometric plate reader at an optical density 630nm. 10 µl of the standards or samples were added to the 96-well plate. 100 µl of the urease/Ammonia Reagent (40 mg of urease for 10 mL of Ammonia reagent) mixture was added to each well. The plate was mixed and incubated for 10 minutes at 37°C. After incubation, 100 µl of the Developing Reagent was added to each well using a multichannel pipette. The plate was placed on an orbital shaker to mix the samples and then incubated 30 minutes at 37°C. After incubation period the plate was read at 630 nm.

### Measurement of sirtuin 1 levels

SIRT1 levels were quantified using SIRT1 Sandwich Enzyme Immunoassay from Mybiosource (Cat # MBS2023445). This kit includes a 96-well strip plate pre-coated with an antibody specific to SIRT1. 100 µl of standards or samples were added to the plate wells with a biotin-conjugated antibody specific to SIRT1 and incubated for

2 hours at 37°C. 100 µl of Detection Reagent A working solution was added to each well and the plate covered and incubated for 1 hour at 37°C. After the incubation period the plate was washed three times with 350 µl of wash solution for each well usingmulti-channel pipette. The plate was allowed to sit for 2 minutes and excess liquid was removed by pressing the plate onto absorbent paper towels. 100 µl of Detection Reagent B working solution was then added to each well and the covered plate was incubated for 30 minutes at 37°C. The plate was then washed with 350 µl of wash solution five times. 90 µl of Tetramethylbenzidine (TMB) Substrate Solution was then added to each well (samples turned blue) and the covered well plate was incubated for 15 minutes at 37°C. The plate was protected from light. 50 µL of Stop Solution was added to each well to stop the reaction and the plate was placed on a shaker to mix the samples well. A microplate reader was used to measure the OD readings of the standards and samples at 450 nm.

### Measurement of AMPK-P levels

The AMPK-P levels in the samples were quantified using an AMPKα pT172 ELISA Kit (Cat # ab154468). This kit contains a 96 well plate which is pre-coated with a specific mouse monoclonal antibody specific for AMPKα pT172. 25 µl of standards (Hek293T cells) or samples were added to the wells along with the rabbit monoclonal primary detector antibody and the plate was incubated for three hours at room temperature. The plate was then washed with 300 µl of 1X wash buffer to eliminate any unbound standard or samples in the plate. After washing and drying of the plate, 50 µl of horseradish peroxidase (HRP)- conjugated secondary detector antibody (HRP Label) specific for the primary detector antibody was added to wells. After incubation, the well plate was washed again three times using 300 µl of 1X wash buffer. Then 100 µl of a Tetramethylbenzidine (TMB) substrate solution was added to the wells and the wells changed in color depending on the amount of AMPKα pT172 bound present in the samples. The OD of the samples was then measured at 600 nm and used to calculate the amount of each AMPK-P in each sample. A standard curve was created and the unknown samples were extrapolated this standard curve.

### Statistical analysis

For the statistical analysis of experiments, we used Graphpad Instat Software (Graphpad, La Jolla, CA, USA). Statistical comparisons between two-groups were performed using the unpaired Student's t-test. All data are mean ± SD represented by the error bars. Means were considered significantly different when $p<0.05$.

## Results

### THS exposure leads to increased oxidative stress in the liver

Previously, we showed that 30% of the mice exposed to THS toxins develop a fatty liver [23]. We hypothesize that exposure to THS toxins leads to lipid accumulation in the liver of THS-exposed mice by increasing oxidative stress. Under normal conditions, the hepatocytes balance oxidative stress with the help of two important antioxidant enzymes, catalase and glutathione peroxidase (GPx). These enzymes regulate the levels of hydrogen peroxide ($H_2O_2$) in the liver. Catalase converts $H_2O_2$ into water and oxygen whereas GPx converts it into water only (Figure 1A).

THS-exposed mice have higher superoxide dismutase (SOD) activity and as a result they also have higher levels of $H_2O_2$ in the liver than do the controls (Figures 1B and 1C). Because there is no significant increase in catalase or GPx activity, $H_2O_2$ is not properly been processed and the levels of reactive oxygen species (ROS) remain high in the liver (Figures 1D and 1E). To further support these results, we measured the $NADP^+/NADPH$ ratio, which is an indicator of the cell reducing potential, because GPx activity is coupled to the reduction of NADPH to NADP+. The NADP+/NADPH ratio is significantly lower in THS-exposed mice than in control mouse livers (Figure 1F), showing that the reduction potential of these animals is decreased and might result in their inability to reduce the oxidative stress levels induced by the THS toxins.

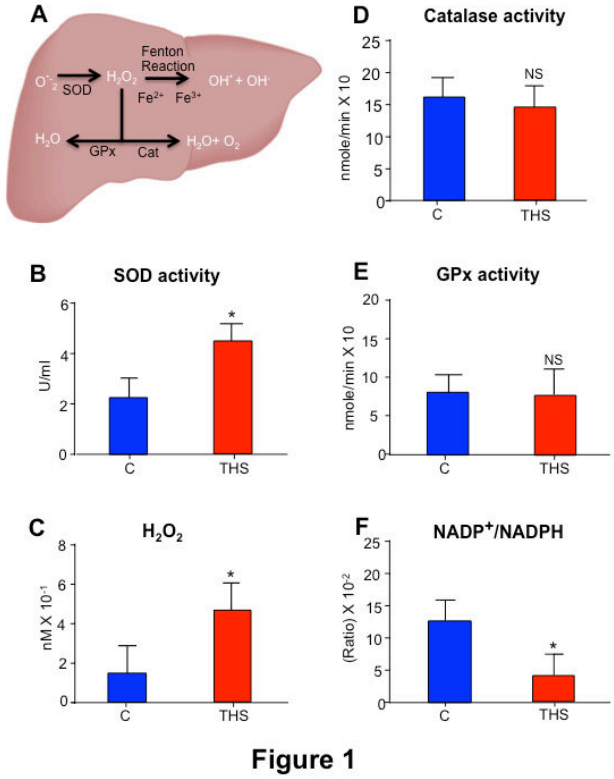


**Figure 1**

**Figure 1:** THS exposure results in oxidative stress in the liver. (A) Simplified schematic representation of the oxidative stress response in cells. When compared with the control, THS exposed mice have increased SOD enzymatic activity (B) increased hydrogen peroxide (C) show significant decrease in catalase enzymatic activity (D) show a significant difference in GPx activity (E) and have a significant decrease of NADP+/NADPH ratio (F). All data are Mean ± SD; *= $p<0.05$; NS= Not statistically significant. n=6. P values were adjusted for the number of times each test was run.

### THS-induced ROS lead to molecular and cellular damage in the liver

High levels of $H_2O_2$ in cells can lead to the production of hydroxyl radicals via the Fenton reaction in the presence of ferrous iron ion ($Fe^{2+}$) (Figure 2A). These radicals can damage lipids and proteins, and lead to the formation of DNA adducts. We found that in the liver of

THS-exposed mice there is significantly higher levels of lipid peroxidation, protein nitrosylation and DNA damage (Figures 2B and 2D). We also investigated whether THS toxins result in functional damage in the liver by measuring ATP, aspartate aminotransferase (AST) and urea levels. ATP is a marker for mitochondria function whereas AST and urea are markers of liver health. THS-exposed mice produced lower ATP levels than the controls (Figure 2E), suggesting that the ability of the mitochondria in THS-exposed mice to synthesize cellular energy is decreased. High levels of AST suggest liver damage whereas high levels of urea suggesting increase in amino acid metabolism (Figures 2F and 2G). Together, these results show that THS toxins result in damage of liver function.

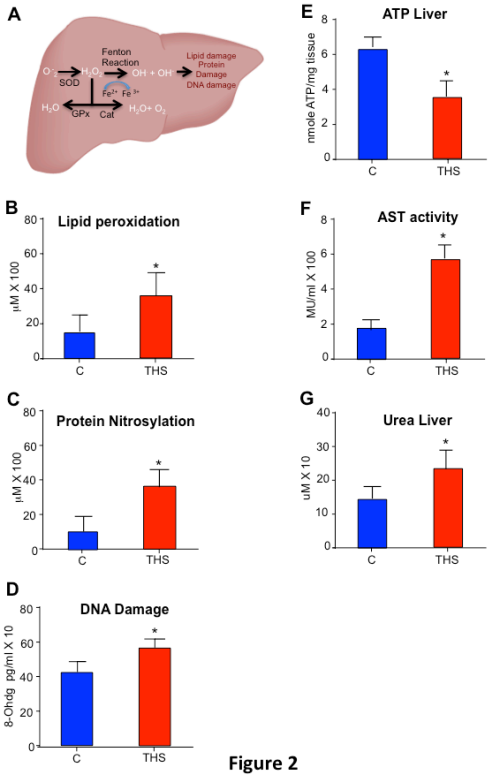


Figure 2

**Figure 2:** THS exposure increase oxidative stress mediated damage in the liver. (A) Model of oxidative stress induced mediated damage in cells. When compared to the control, THS exposed mice have higher lipid peroxidation (B) higher protein nitrosylation (C) higher DNA damage (D) decreased ATP levels (E) increased AST levels (F) and increased urea levels (G). All data are Mean ± SD *= p<0.05 NS= Not statistically significant. n=8 for B,C, and D. n=6 for E-G. P values were adjusted for the number of times each test was run.

## Oxidative stress mediated damage is improved by treating the mice with antioxidants

To investigate whether the THS-induced oxidative stress in the liver can be reversed, we treated the THS-exposed mice with the antioxidants N-acetylcysteine (NAC) and α-tocopherol (α-TOC) for five months. These two antioxidants have been used previously to treat oxidative stress in different tissues [37-39]. Treatment with these antioxidants for five months while the mice were being exposed to THS, leads to a decrease in oxidative stress. These mice have SOD activity and $H_2O_2$ levels similar to those of the non-exposed mice treated with antioxidants but significantly lower than THS-exposed mice without treatment with antioxidants (Figures 3A and 3B). Although no significant changes were observed in the activity of catalase (Figure 3C), the THS-exposed mice treated with antioxidants have higher GPx activity than THS-exposed non-treated mice (Figure 3D). The same occurred for the $NADP^+$/NADPH ratio (Figure 3E). Furthermore, NAC and α-TOC lowered the total hepatic lipid weight in the THS-exposed mice (Figure 3F).

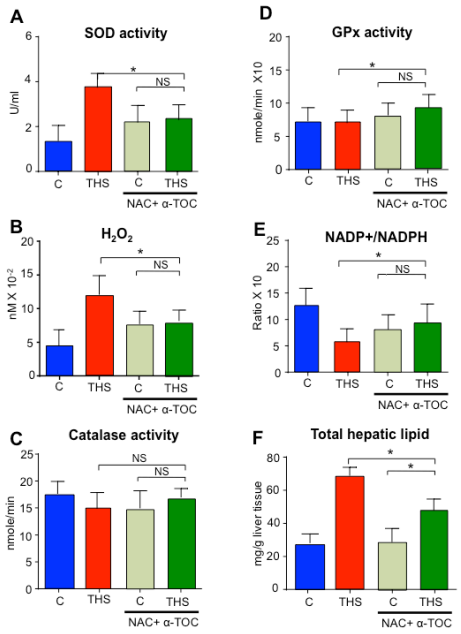


Figure 3

**Figure 3:** Antioxidant treatment leads to improvement of oxidative stress in the liver of THS-exposed mice. THS-exposed mice treated with the NAC+ α-TOC have significantly reduced of SOD activity (A), lower levels of $H_2O_2$ (B), no significant change in the enzymatic activity of catalase (C), significant change in the enzymatic activity of GPx (D), significant increase of $NADP^+$/NADPH ratio (E) and in significant lowering of total hepatic lipid weight (F). All data are Mean ± SD *= p<0.05 NS= Not statistically significant n=9 for A and E n=8 for B,C, and D. n=6 for F. P values were adjusted for the number of times each test was run.

Treatment with antioxidant agents also decreased the oxidative-stress-mediated molecular damage in THS-exposed mice. These mice have lower lipid peroxidation (Figure 4A) and lower protein damage (Figure 4B) in THS exposed mice. However, no significant

improvement was observed in DNA damage (Figure 4C). We also investigated whether antioxidant treatment improved functional damage by measuring ATP, AST and urea. AST is responsible for the conversion of aspartate to α-ketoglutarate to oxaloacetate and glutamate, which is fundamental for the function of the liver. Urea is a by-product of amino acid metabolism that occurs in the liver. Antioxidant treatment did not improve these parameters (Figures 4D and 4F).

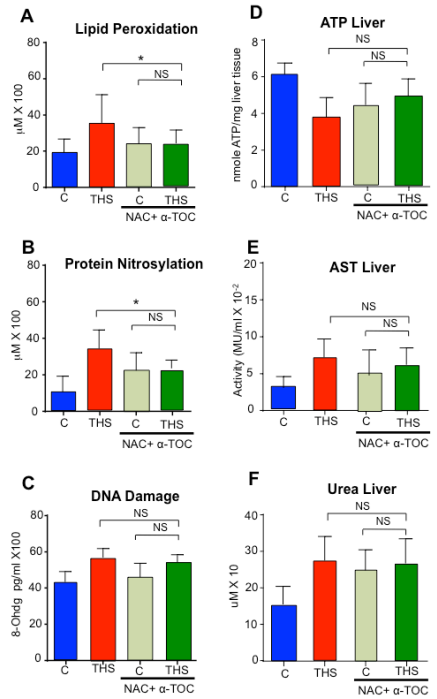


Figure 4

**Figure 4:** Oxidative stress mediated damage is improved by treating the mice with antioxidants. THS-exposed mice treated with NAC+ α-TOC show lower lipid peroxidation (A) lower protein nitrosylation but (B) no significant difference in DNA damage (C), ATP levels (D), AST levels (E) or urea levels (F). All data are Mean ± SD *= $p<0.05$, NS= Not statistically significant. n=8 for A n=7 for B n=9 for C, D E, F. P values were adjusted for the number of times each test was run.

## Treatment of THS-exposed mice with APAP increases oxidative-stress-mediated damage

Because N-acetyl-p-aminophenol (APAP/Tylenol) is a common drug taken by many people, especially by children, and it is known to damage the liver if taken in high doses [40], we investigated whether giving THS-exposed mice Tylenol would further increase oxidative stress in the liver. We used a dose the APAP/Tylenol that has been previously shown to induce chemical damage in the liver without killing the animals [40-42]. Based on these studies, we treated the THS-exposed mice for eight weeks with APAP/Tylenol. THS-exposed mice treated with APAP/Tylenol have higher SOD activity and higher $H_2O_2$ levels than THS-exposed non-treated mice (Figures 5A and 5B). Moreover, the levels of catalase activity were significantly decreased when compare with THS exposed non-APAP treated animals (Figure 5C). We also observed that although GPx activity was not changed (Figure 5D), the $NADP^+$/NADPH ratio was signi icantly decreased (Figure 5E), showing that the reducing potential in the THS-exposed APAP-treated mice was low. Furthermore, APAP/Tylenol increased the total hepatic lipid weight in the THS-exposed mice (Figure 5F). This, results in further damage to the ability of the liver to handle the oxidative stress damage induced by THS.

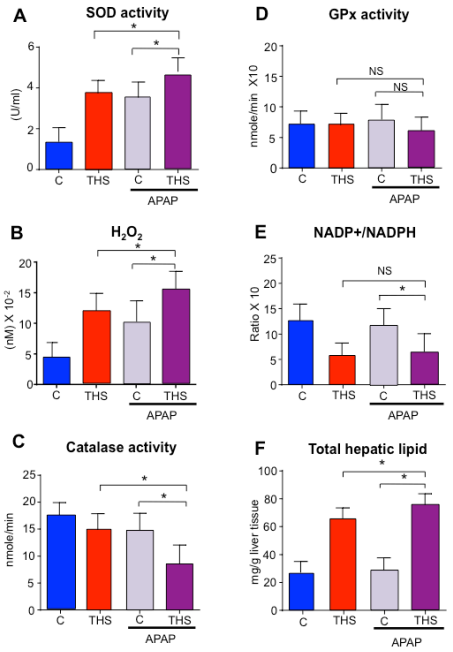


Figure 5

**Figure 5:** APAP treatment results in increased oxidative stress in THS-exposed mice. APAP treatment of THS-exposed mice results in higher SOD activity (A) higher levels of hydrogen peroxide (B) decrease in catalase activity (C) but no significant change in GPx activity (D). APAP treatment also did not have a signi icant impact in the $NADP^+$/NAPPH ratio (F) but resulted in higher total lipid hepatic weight in THS-exposed mice. All data are Mean ± SD *= $p<0.05$ NS= Not statistically significant n=9 for A and E n=8 for B,C, D. n=6 for F. P values were adjusted for the number of times each test was run.

We also quantified the oxidative stress-induced molecular damage and observed that THS exposure in conjunction with APAP/Tylenol treatment results in much higher levels of lipid peroxidation (Figure 6A), higher protein nitrosylation (Figure 6B) and higher DNA damage (Figure 6C). In addition, we also measured the ATP, AST and urea levels. High levels of AST and urea are associated with abnormal liver

function [43,44]. APAP treatment results in lower ATP levels in THS-exposed mice suggesting that these mice have dysfunctional mitochondria (Figure 6D). APAP/Tylenol treatment results in higher AST levels in these animals suggesting that when THS exposure and APAP/Tylenol treatment are combined, further functional damage to the liver occurs (Figure 6E). However, APAP/Tylenol treatment of the THS-exposed mice did not have increased urea levels when compared to exposure only to THS (Figure 6F).

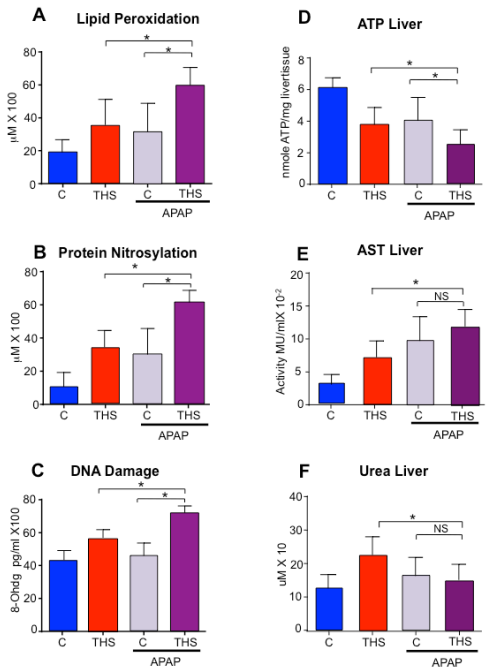


Figure 6

**Figure 6:** THS-exposed mice treated with APAP show increased oxidative stress mediated damage. APAP treatment results in higher lipid peroxidation (A), higher protein nitrosylation (B), and higher DNA damage (C) in the liver of THS-exposed mice. THS-exposed mice treated with APAP also have lower ATP levels (D) higher AST levels but (E) and lower urea levels (D) than THS-exposed mice. All data are Mean ± SD *= $p<0.05$, NS= Not statistically significant. n=8 for A n=7 for B n=9 for C,D E,F. P values were adjusted for the number of times each test was run.

## THS toxins inhibit the SIRT1/AMPK/ SBREP1c signaling pathway in the liver

To investigate the cellular and molecular mechanisms of THS-induced lipid metabolism, we performed genomic analysis using both DNA microarray and RNA-Seq and found that Sirtuin 1 (SIRT1), a key regulator of lipid metabolism, is down regulated in THS-exposed mice. SIRT1 modulates the activity of other metabolic energy regulators such as 5' AMP-activated protein kinase (AMPK). AMPK is an energy sensor within the cell that responds to energy depletion (decrease in ATP production) or any other cellular damage insult that result in alterations to cellular energy. Together, SIRT1 and AMPK regulate lipid metabolism by preventing the synthesis of lipids and by stimulating fatty acid oxidation [45-59]. It has been shown using SIRT1 transgenic mice showed SIRT1 is required for activation of that AMPK and improvement of mitochondrial function [58]. It has also been shown AMPK phosphorylates and inhibits SREBP1c in diet induced insulin resistant mice [59]. Taken together studies suggest that SIRT1 and AMPK both work to prevent abnormal lipid metabolism by targeting and inhibiting SREBP1c a key lipogenic enzyme in the liver. Therefore, we investigated the SIRT1/AMPK/SREBP1c pathway and the THS-induced hepatic steatosis is a result of alterations in this pathway. When compared to the control mice the THS-exposed animals have lower levels of SIRT1 and of phosphorylated AMPK, the active form of this enzyme (Figures 7A and 7B).

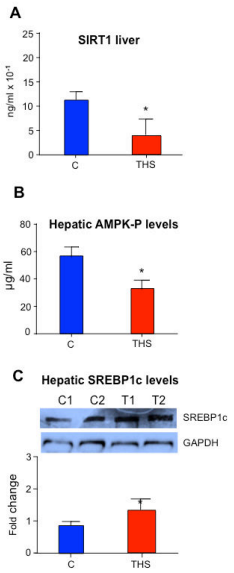


Figure 7

**Figure 7:** THS toxins alter the SIRT1/AMPK/ SBREP1c signaling in the liver. Compared to the control, THS-exposed mice have lower levels of SIRT1 (A), lower level of pAMPK (B) and higher levels of SREBP1c (C). *= $p<0.05$, ** $p<0.01$ NS= Not statistically significant. n=6 P values were adjusted for the number of times each test was run. "Fold change" on western blot quantification graph indicates fold change to control.

Because activated AMPK is decreased in THS-exposed mice we tested the levels of SREBP1c the levels of SREBP1c. We found that in THS-exposed mice SREBP1c is elevated, leading to higher levels of lipids in the liver (Figure 7C). These findings suggest that THS exposure stimulate hepatic steatosis by altering the SIRT1/AMPK/ SREBP1c pathway.

## Discussion

We have previously shown that THS exposure results in the damage of multiple organs in mice including steatosis of the liver [23]. Here we show that the lipid accumulation is due to increase in the levels of oxidative stress, primarily of ROS, and inhibition of the SIRT1/AMPK/SREBP1c pathway (Figure 8A). Modulating the levels of ROS with antioxidants resulted in improvement of the THS-induced hepatic steatosis whereas treatment with APAP resulted in augmentation of the THS-induced the lipid accumulation (Figure 8B).

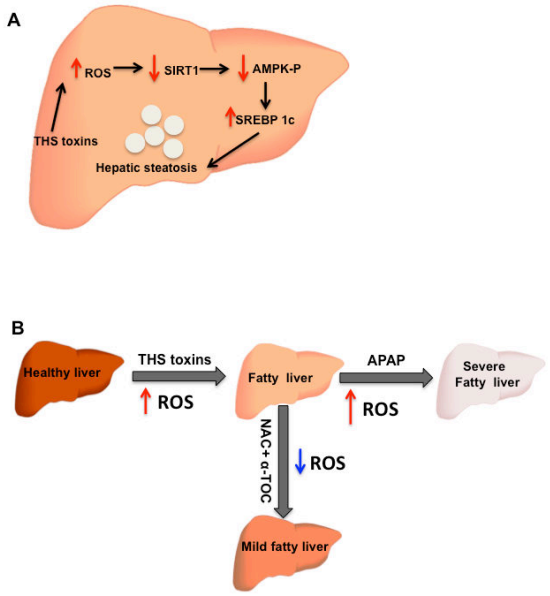


**Figure 8**

**Figure 8:** Proposed model for THS-induced hepatic steatosis. (A) A schematic representation of THS-induced hepatic steatosis in mice depicting a pathway by which THS toxins increase oxidative stress in the liver, which results in decrease of SIRT1 levels, a key regulator oxidative stress and regulator of lipid metabolism. The toxins also result in a decrease in the levels of active/phosphorylated AMPK and increase in SREBP1c levels, a stimulator of de novo lipid synthesis. As a result THS exposure stimulates fat accumulation in the liver resulting in hepatic steatosis. (B) A schematic summarizing THS-induced oxidative stress and fatty liver. Increasing oxidative stress by treating THS-exposed mice with APAP leads to severe fatty liver disease while decreasing oxidative stress by treating the mice with NAC+ α- TOC results in reducing fatty liver.

The oxidative stress mediated damage to the hepatic lipids, proteins, and DNA have a detrimental effect for lipid metabolism [60-62]. The liver is one of the major metabolic organs where glucose is metabolized, modified and stored. Perturbations in the metabolism and storage of glucose as well as insulin resistance in the liver have been linked to the development of hepatic steatosis [63,64]. It is known that lipid peroxidation results in a decrease in the uptake of glucose in cortical rat neurons, which in the short term leads to abnormal glucose metabolism but over time it may lead to cell death [65]. Lipid peroxidation can also lead to conformational changes in the lipid bilayer and these changes can potentially alter the localization and stability of many receptors involved in lipid metabolism [66].

THS-exposed mice have high levels of protein damage, which affect the expression, and levels of proteins involved in the regulation of lipid metabolism in the liver. SIRT1 is a key regulator of lipid metabolism and it is known to work together with AMPK to prevent lipid accumulation in the liver by inhibiting SREBP1c and increasing fatty acid metabolism [46-59]. In this study we show that THS toxins alter the SIRT1/AMPK/SREBP1c signaling axis by decreasing SIRT1 levels which lead to decrease in phosphorylated/activated AMPK resulting in increase of SREBP1c and increase in lipid synthesis, with subsequent development of hepatic steatosis (Figure 8A). We also show that the liver specific damage we observed in the THS-exposed mice is mediated by oxidative stress triggered by the THS toxins. Increasing the oxidative stress in the liver of THS-exposed mice with APAP/Tylenol worsened lipid accumulation whereas when the mice were exposed to THS and treated with antioxidants there was a decrease in lipid accumulation.

APAP/Tylenol is commonly used to treat headaches and fever and when taken for prolonged periods of time or higher dose it is known to cause liver damage. This can occur by depletion of glutathione (GSH) and by increasing mitochondria damage [67-69]. When we treated THS-exposed mice with APAP, we observed that these mice have higher liver damage than mice only exposed to THS. These mice also have lower levels of ATP, which suggest impaired mitochondria function. AST levels were also elevated suggesting abnormality in amino acid metabolism in the liver.

To decrease oxidative stress we treated THS-exposed mice with NAC and α-TOC that have been commonly used in humans and rodents for that purpose [70-72]. NAC is derivative of the amino acid L-cysteine and it is a direct precursor of glutathione consequently it has direct and indirect antioxidant properties [71]. Its free thiol group can interact with the electrophilic groups found in reactive oxygen species (ROS) agents. NAC can behave as an indirect antioxidant in the glutathione synthesis pathway, an antioxidant enzyme that decreases cellular oxidative stress [71]. α-TOC is an important lipid-soluble antioxidant that reacts with lipid radicals and consequently less lipid peroxidation occurs preventing damage to the plasma and mitochondrial membranes [72].

In conclusion, these studies provide insight into the effects of THS toxins on key molecules in lipid metabolism such as the SIRT1/AMPK/SIRT1 signaling pathway. We show that by altering the oxidative stress levels using APAP/tylenol or the antioxidant agents NAC and a-TOC, we alter the THS-induced damage, which indicates that the THS-induced damage is mediated by oxidative stress. Based on our results, it is clear that THS toxins have the ability to alter fundamental metabolic processes such as lipid metabolism resulting in steatosis making THS a new risk factor for hepatic steatosis.

## References

1. Winickoff JP, Friebely J, Tanski SE, Sherrod C, Matt GE, et al. (2009) Beliefs about the health effects of "thirdhand" smoke and home smoking bans. Pediatrics 123: e74-e79.

2. Burton A (2011) Does the smoke ever really clear? Thirdhand smoke exposure raises new concerns. Environ Health Perspect 119: A70-A74.
3. Whitehead T, Metayer C, Ward MH, Nishioka MG, Gunier R, et al. (2009). Is house-dust nicotine a good surrogate for household smoking?. Am J Epidemiol 169: 1113-1123.
4. Sleiman M, Gundel LA, Pankow JF, Jacob P, Singer, BC, et al. (2010) Formation of carcinogens indoors by surface-mediated reactions of nicotine with nitrous acid, leading to potential thirdhand smoke hazards. Proc Natl Acad Sci USA 107: 6576-6581.
5. Van Loy MD, Riley WJ, Daisey JM, Nazaroff WW (2001) Dynamic behavior of semivolatile organic compounds in indoor air. 2. Nicotine and phenanthrene with carpet and wallboard. Environ Sci Technol 35: 560-567.
6. Caldwell WS, Greene JM, Plowchalk DR, DeBethizy JD (1991) The nitrosation of nicotine: a kinetic study. Chem Res Toxicol 4: 513-516.
7. Singer BC, Revzan KL, Hotchi T, Hodgson AT, Brown NJ (2004) Sorption of organic gases in a furnished room. Atmos Environ 38: 2483-2494.
8. Sleiman M, Destaillats H, Smith JD, Liu CL, Ahmed M (2010) Secondary organic aerosol formation from ozone-initiated reactions with nicotine and secondhand tobacco smoke. Atmos Environ 44: 4191-4198.
9. Hoffmann D, Brunnemann KD, Prokopczyk B, Djordjevic MV (1994) Tobacco-specific N-nitrosamines and ARECA-derived N-nitrosamines: Chemistry, biochemistry, carcinogenicity, and relevance to humans. J Toxicol Environ Health 41: 1-52.
10. Hecht SS (1998) Biochemistry, biology, and carcinogenicity of tobacco-specific N-nitrosamines. Chem Res Toxicol 11: 559-603.
11. Matt GE, Quintana PJE, Hovell MF, Bernert JT, Song S, et al. (2004) Households contaminated by environmental tobacco smoke: sources of infant exposures. Tob Control 13: 29-37.
12. Centers for Disease Control and Prevention (2011) Smoking and Tobacco Use: Data and Statistics.
13. Hecht SS, Carmella SG, Le KA, Murphy SE, Boettcher AJ, et al. (2006) 4-(methylnitrosamino)-1-(3-pyridyl)-1-butanol and its glucuronides in the urine of infants exposed to environmental tobacco smoke. Cancer Epidemiol Biomarkers Prev 15: 988-992.
14. Singh GK, Siahpush M, Kogan MD (2010) Disparities in children's exposure to environmental tobacco smoke in the United States, 2007. Pediatrics 2009-2744.
15. Thomas JL, Guo H, Carmella SG, Balbo S, Han S, et al. (2011) Metabolites of a tobacco-specific lung carcinogen in children exposed to secondhand or thirdhand tobacco smoke in their homes. Cancer Epidemiol Biomarkers Prev 20: 1213-1221.
16. Hang B, Sarker AH, Havel C, Saha S, Hazra TK, et al. (2013) Thirdhand smoke causes DNA damage in human cells. Mutagenesis 28: 381-391.
17. Roberts JW, Dickey P (1995) Exposure of children to pollutants in house dust and indoor air. Rev Environ Contam Toxicol 143: 59-78.
18. Xu B, Chen M, Yao M, Ji X, Mao Z, et al. (2015) Metabolomics reveals metabolic changes in male reproductive cells exposed to thirdhand smoke. Sci Rep 6.
19. Rehan VK, Sakurai R, Torday JS (2011) Thirdhand smoke: a new dimension to the effects of cigarette smoke on the developing lung. Am J Physiol Lung Cell Mol Physiol 301: L1-L8.
20. Yolton K, Dietrich K, Auinger P, Lanphear BP, Hornung R (2005) Exposure to environmental tobacco smoke and cognitive abilities among US children and adolescents. Environ Health Perspect 2005:9 8-103.
21. Elliot J, Vullermin P, Robinson P (1998) Maternal cigarette smoking is associated with increased inner airway wall thickness in children who die from sudden infant death syndrome. Am J Respir Crit Care Med 158: 802-806.
22. Jung JW, Ju YS, Kang HR (2012) Association between parental smoking behavior and children's respiratory morbidity: 5-year study in an urban city of South Korea. Pediatr pulmonol 47: 338-345.
23. Martins-Green M, Adhami N, Frankos M, Valdez M, Goodwin B, et al. (2014) Cigarette smoke toxins deposited on surfaces: implications for human health. PloS one 9: E86391.
24. Adhami N, Starck SR, Flores C, Green MM (2016) A Health Threat to Bystanders Living in the Homes of Smokers: How Smoke Toxins Deposited on Surfaces Can Cause Insulin Resistance. PloS one 11: e0149510.
25. Erickson SK (2009) Nonalcoholic fatty liver disease. lipid res 50: S412-S416.
26. Marrero JA, Fontana RJ, Su GL, Conjeevaram HS, Emick DM, et al. (2002) NAFLD may be a common underlying liver disease in patients with hepatocellular carcinoma in the United States. Hepatology 36: 1349-1354.
27. Cazanave SC, Sanyal AJ (2016) Molecular Mechanisms of Lipotoxicity in Nonalcoholic Fatty Liver Disease. In Hepatic De Novo Lipogenesis and Regulation of Metabolism. Springer International Publishing.
28. Tiniakos DG, Vos MB, Brunt EM (2010) Nonalcoholic fatty liver disease: pathology and pathogenesis. Annu Rev Pathol 5: 145-171.
29. Letteron P, Sutton A, Mansouri A, Fromenty B, Pessayre D (2003) Inhibition of microsomal triglyceride transfer protein: Another mechanism for drug-induced steatosis in mice. Hepatology 38: 133-140.
30. Fromenty B, Pessayre D (1997) Impaired mitochondrial function in microvesicular steatosis effects of drugs, ethanol, hormones and cytokines. J Hepatol 26: 43-53.
31. Azzalini L, Ferrer E, Ramalho LN, Moreno M, Domínguez M, et al. (2010) Cigarette smoking exacerbates nonalcoholic fatty liver disease in obese rats. Hepatology 51: 1567-1576.
32. Browning JD, Horton JD (2004) Molecular mediators of hepatic steatosis and liver injury. J Clin Invest 114: 147-152.
33. Tolosa L, Gómez-Lechón MJ, Jiménez N, Hervás D, Jover R, et al. (2016) Advantageous use of HepaRG cells for the screening and mechanistic study of drug-induced steatosis. Toxicol Appl Pharmacol.
34. Petersen KF, Dufour S, Befroy D, Lehrke M, Hendler RE, et al. (2005) Reversal of nonalcoholic hepatic steatosis, hepatic insulin resistance, and hyperglycemia by moderate weight reduction in patients with type 2 diabetes. Diabetes 54: 603-608.
35. Ryan MC, Itsiopoulos C, Thodis T, Ward G, Trost N, et al. (2013) The Mediterranean diet improves hepatic steatosis and insulin sensitivity in individuals with non-alcoholic fatty liver disease. J Hepatol 59: 138-143.
36. Faghihzadeh F, Adibi P, Rafiei R, Hekmatdoost A (2014) Resveratrol supplementation improves inflammatory biomarkers in patients with nonalcoholic fatty liver disease. Nutr Res 34: 837-843.
37. de Diego-Otero Y, Romero-Zerbo Y, el Bekay R, Decara J, Sanchez L, et al. (2009) α-tocopherol protects against oxidative stress in the fragile X knockout mouse: an experimental therapeutic approach for the Fmr1 deficiency. Neuropsychopharmacology 34: 1011-1026.
38. Thakurta IG, Banerjee P, Bagh MB, Ghosh A, Sahoo A, et al. (2014) Combination of N-acetylcysteine, α-lipoic acid and α-tocopherol substantially prevents the brain synaptosomal alterations and memory and learning deficits of aged rats. Exp Gerontol 50: 19-25.
39. Joseph, AJ, Adamu, KB, Shu'aibu Yahya BRL, Martina BS, Asabe MUA, et al. (2014) Influence of high dietary vitamin C and E oral administration on anemia and organ damage in wistar rat infected with Trypanosoma brucei brucei (Federe strain).
40. Jaw S, Jeffery EH (1993) Interaction of caffeine with acetaminophen: 1. Correlation of the effect of caffeine on acetaminophen hepatotoxicity and acetaminophen bioactivation following treatment of mice with various cytochrome P450 inducing agents. Biochemical pharmacology 46: 493-501.
41. Zaher H, Buters JT, Ward JM, Bruno, MK, Lucas AM, et al. (1998) Protection against acetaminophen toxicity in CYP1A2 and CYP2E1 double-null mice. Toxi appl pharm 152: 193-199.
42. Shayiq RM, Roberts DW, Rothstein K, Snawder JE, Benson W, et al. (1999) Repeat exposure to incremental doses of acetaminophen provides protection against acetaminophen-induced lethality in mice: An explanation for high acetaminophen dosage in humans without hepatic injury. Hepatology 29: 451-463.

43. Abdel-Daim MM, Abuzead, SM, Halawa SM (2013) Protective role of Spirulina platensis against acute deltamethrin-induced toxicity in rats. PLoS One 8: e72991.
44. Puche JE, Lee YA, Jiao J, Aloman C, Fiel MI, et al. (2013) A novel murine model to deplete hepatic stellate cells uncovers their role in amplifying liver damage in mice. Hepatology 57: 339-350.
45. Caito S, Rajendrasozhan S, Cook S, Chung S, Yao H, et al. (2010) SIRT1 is a redox-sensitive deacetylase that is post-translationally modified by oxidants and carbonyl stress.
46. Merksamer PI, Liu Y, He W, Hirschey MD, Chen D, et al. (2013) The sirtuins, oxidative stress and aging: an emerging link. Aging 5: 144-150.
47. Purushotham A, Schug TT, Xu Q, Surapureddi S, Guo X, et al. (2009) Hepatocyte-specific deletion of SIRT1 alters fatty acid metabolism and results in hepatic steatosis and inflammation. Cell metab 9: 327-338.
48. Brunet A, Sweeney LB, Sturgill JF, Chua, KF, Greer PL, et al. (2004) Stress-dependent regulation of FOXO transcription factors by the SIRT1 deacetylase. Science 303: 2011-2015.
49. Webster BR, Lu Z, Sack MN, Scott I (2012) The role of sirtuins in modulating redox stressors. Free Radic Biol Med 52: 281-290.
50. Chen WL, Kang CH, Wang SG, Lee HM (2012) α-Lipoic acid regulates lipid metabolism through induction of sirtuin 1 (SIRT1) and activation of AMP-activated protein kinase. Diabetologia 55: 1824-1835.
51. Walker AK, Yang F, Jiang K, Ji JY, Watts JL, et al. (2010) Conserved role of SIRT1 orthologs in fasting-dependent inhibition of the lipid/cholesterol regulator SREBP. Genes & development 24: 1403-1417.
52. Rodgers JT, Puigserver P (2007) Fasting-dependent glucose and lipid metabolic response through hepatic sirtuin 1. Proc Natl Acad Sci USA 104: 12861-12866.
53. Ponugoti B, Kim DH, Xiao Z, Smith Z, Miao J, et al. (2010) SIRT1 deacetylates and inhibits SREBP-1C activity in regulation of hepatic lipid metabolism. J Biol Chem 285: 33959-33970.
54. Kim E, Choi Y, Jang J, Park T (2013) Carvacrol protects against hepatic steatosis in mice fed a high-fat diet by enhancing SIRT1-AMPK signaling. Evid Based Complement Alternat Med 2013: 290104.
55. Yuan H, Shyy JYJ, Martins-Green M (2009) Second-hand smoke stimulates lipid accumulation in the liver by modulating AMPK and SREBP-1. J Hepatol 51: 535-547.
56. Jung EJ, Kwon SW, Jung BH, Oh SH, Lee BH (2011) Role of the AMPK/SREBP-1 pathway in the development of orotic acid-induced fatty liver. J Lipid Res 52: 1617-1625.
57. Ahmed MH, Byrne CD (2007) Modulation of sterol regulatory element binding proteins (SREBPs) as potential treatments for non-alcoholic fatty liver disease (NAFLD). Drug Discov Today 12: 740-747.
58. Price NL, Gomes AP, Ling AJ, Duarte FV, Martin-Montalvo A, et al. (2012) SIRT1 is required for AMPK activation and the beneficial effects of resveratrol on mitochondrial function. Cell metab 15: 675-690.
59. Li Y, Xu S, Mihaylova MM, Zheng B, Hou X, et al. (2011) AMPK phosphorylates and inhibits SREBP activity to attenuate hepatic steatosis and atherosclerosis in diet-induced insulin-resistant mice. Cell Metab 13: 376-388.
60. Seki S, Kitada T, Yamada T, Sakaguchi H, Nakatani K, et al. (2002) In situ detection of lipid peroxidation and oxidative DNA damage in non-alcoholic fatty liver diseases. Journal of hepatology 37: 56-62.
61. Pan M, Cederbaum AI, Zhang YL, Ginsberg HN, Williams KJ, et al. (2004) Lipid peroxidation and oxidant stress regulate hepatic apolipoprotein B degradation and VLDL production. J Clin Invest 113: 1277-1287.
62. Bryant RJ, Ryder J, Martino P, Kim J, Craig BW (2003) Effects of vitamin E and C supplementation either alone or in combination on exercise-induced lipid peroxidation in trained cyclists. J Strength Cond Res 17: 792-800.
63. Flannery C, Dufour S, Rabøl R, Shulman GI, Petersen KF (2012) Skeletal muscle insulin resistance promotes increased hepatic de novo lipogenesis, hyperlipidemia, and hepatic steatosis in the elderly. Diabetes 61: 2711-2717.
64. Perry R J, Samuel VT, Petersen KF, Shulman GI (2014) The role of hepatic lipids in hepatic insulin resistance and type 2 diabetes. Nature 510: 84-91.
65. Lovell MA, Xie C, Markesbery WR (2000) Acrolein, a product of lipid peroxidation, inhibits glucose and glutamate uptake in primary neuronal cultures. Free Radic Biol Med 29: 714-720.
66. Catalá A (2012) Lipid peroxidation modifies the picture of membranes from the "Fluid Mosaic Model" to the "Lipid Whisker Model". Biochimie 94: 101-109.
67. Reid AB, Kurten RC, McCullough SS, Brock RW, Hinson JA (2005) Mechanisms of acetaminophen-induced hepatotoxicity: role of oxidative stress and mitochondrial permeability transition in freshly isolated mouse hepatocytes. J Pharmacol Exp Ther 312: 509-516.
68. Xie Y, McGill MR, Dorko K, Kumer SC, Schmitt TM, et al. (2014) Mechanisms of acetaminophen-induced cell death in primary human hepatocytes. Toxi Appli pharm 279: 266-274.
69. McGill MR, Sharpe MR, Williams CD, Taha M, Curry SC, et al. (2012) The mechanism underlying acetaminophen-induced hepatotoxicity in humans and mice involves mitochondrial damage and nuclear DNA fragmentation. J Clin Invest 122: 1574-1583.
70. Mehta K, Van Thiel DH, Shah N, Mobarhan S (2002) Nonalcoholic fatty liver disease: pathogenesis and the role of antioxidants. Nutr Rev 60: 289-293.
71. Grinberg L, Fibach E, Amer J, Atlas D (2005) N-acetylcysteine amide, a novel cell-permeating thiol, restores cellular glutathione and protects human red blood cells from oxidative stress. Free Radic Biol Med 38: 136-145.
72. Niki E (2014) Role of vitamin E as a lipid-soluble peroxyl radical scavenger: in vitro and in vivo evidence. Free Radic Biol Med 66: 3-12.